Electron and Lattice Transport Phenomena in an Antimony Crystal at Liquid-He^4 Temperatures*

J. R. LONG,† C. G. GRENIER, AND J. M. REYNOLDS
Department of Physics, Louisiana State University, Baton Rouge, Louisiana
(Received 28 January 1965; revised manuscript received 17 May 1965)

In a very pure single crystal of antimony, a complete set of kinetic transport coefficients of the galvanomagnetic and thermomagnetic effects was determined at each of the temperatures 1.6, 2.1, 3.0, and 4.0°K in fields up to 18 kG. Standard measuring techniques were employed. An electron-phonon normal process was found to dominate the scattering for both electronic and lattice conduction. The usual theories assuming a time of relaxation were applied to the gross coefficients, while the oscillations found at the higher fields were analyzed in terms of the several existing theories which take account of Landau quantization. Both the lattice thermal and ideal electrical conductivities appeared to be anomalous in magnitude and temperature dependence, but their ratio was very satisfactorily fitted to the relation expected for an N process. A standard two-band model assuming a time of relaxation gave remarkably good agreement with data for the field dependence of the gross effects. The magnitude and large temperature dependence of the Nernst-Ettingshausen coefficient were satisfactorily explained by a simple theory of phonon drag. Since the lattice conductivity was limited by electron scattering, the oscillations in the lattice thermal resistivity were quantitatively shown to be a result of an oscillation in the density of scattering centers, as a consequence of Landau quantization.

I. INTRODUCTION

BY the application of a magnetic field to a semimetal it is possible to observe separately some of the metallic properties and some properties of the lattice in a single specimen. For this reason, and as part of a general program in the study of transport effects,[1–4] a set of six independent transport coefficients was measured in a single crystal of the semimetal antimony, from which the kinetic tensors[5,6] were computed. Antimony, like bismuth, is quinquevalent with two atoms per unit cell, thus leading to five filled Brillouin zones. Overlap at the fifth zone boundary results in a description of the transport properties and related phenomena in terms of two bands, one of holes, and one of electrons, each with approximately 1.2×10^{-3} carriers/atom and Fermi energy $\gtrsim10^{-13}$ erg. Recent opinion has been divided between this "classic" description and a three-band model.[7]

Antimony has been extensively studied by de Haas–van Alphen effect,[8–10] Shubnikov–de Haas effect,[4,11] ultrasonic attenuation,[12,13] cyclotron resonance,[14–17] anomalous skin effect,[18] infrared absorption,[19] and galvanomagnetic effects at high[20,21] and low[4,22] temperatures. The magnetothermopowers and thermoresistance effects reported here for liquid-helium temperatures apparently have not been studied since the early work of Rausch.[23]

Models of the band structure resulting from these studies seem to fall into two categories. In each of these, the rather well-known set of three tilted (Shoenberg[8]) ellipsoids are called electrons. The remainder of the carriers are presumed to be an equal number of holes. In one model, these "holes" are described in terms of a set of three (warped?) ellipsoids with only slight tilt[9,10,16] and in the other model the holes are divided into two bands of light and heavy holes corresponding to one prolate and one oblate ellipsoid.[4,7] It should be kept in mind, however, that these models presume the Shoenberg ellipsoids to be electrons and a positive identification as such has not been made.[14,16,21]

Phenomenological definitions, conventions and pertinent experimental facts follow these introductory paragraphs. The results and discussion of each of the separable aspects of the transport phenomena are then given. In Sec. IVA the ideal electrical conductivity and the lattice thermal conductivity are discussed. In IVB

* This work was done under the auspices of the U. S. Atomic Energy Commission and supported in part by the National Science Foundation for the use of the Computer Research Center.
† Present address: School of Metallurgical Engineering, University of Pennsylvania, Philadelphia, Pennsylvania.

[1] C. J. Bergeron, C. G. Grenier, and J. M. Reynolds, Phys. Rev. **119**, 925 (1960).
[2] C. G. Grenier, J. M. Reynolds, and N. H. Zebouni, Phys. Rev. **129**, 1088 (1963).
[3] C. G. Grenier, J. M. Reynolds, and J. R. Sybert, Phys. Rev. **132**, 58 (1963).
[4] G. N. Rao, N. H. Zebouni, C. G. Grenier, and J. M. Reynolds, Phys. Rev. **133**, A141 (1964).
[5] J. P. Jan, Solid State Phys. **5**, 1 (1957).
[6] H. B. Callen, Phys. Rev. **73**, 1349 (1948); **85**, 16 (1952).
[7] J. J. Hall and S. H. Koenig, IBM J. Res. Develop. **8**, 241 (1964).
[8] D. Shoenberg, Phil. Trans. Roy. Soc. (London) **A245**, 1 (1952).
[9] Y. Saito, J. Phys. Soc. (Japan) **18**, 452 (L) (1963).
[10] L. R. Windmiller and M. G. Priestly, Bull. Am. Phys. Soc. **9**, 632 (1964).
[11] J. Ketterson and Y. Eckstein, Phys. Rev. **132**, 1885 (1963).
[12] Y. Eckstein, Phys. Rev. **129**, 12 (1963).
[13] J. Ketterson, Phys. Rev. **129**, 18 (1963).
[14] W. R. Datars and R. N. Dexter, Phys. Rev. **124**, 75 (1961).
[15] W. R. Datars, Can. J. Phys. **39**, 1922 (1961).
[16] W. R. Datars and J. Vanderkooy, IBM J. Res. Develop. **8**, 247 (1964).
[17] G. E. Everett, Bull. Am. Phys. Soc. **9**, 383 (1964).
[18] A. J. Greenfield, G. E. Smith, and A. W. Lawson, Bull. Am. Phys. Soc. **4**, 409 (1959).
[19] C. Nanney, Phys. Rev. **129**, 109 (1963).
[20] S. J. Freedman and H. J. Juretschke, Phys. Rev. **124**, 1379 (1961).
[21] S. Epstein and H. J. Juretschke, Phys. Rev. **129**, 1148 (1963).
[22] M. C. Steele, Phys. Rev. **99**, 1751 (1955).
[23] K. Rausch, Ann. Physik **1**, 190 (1947).

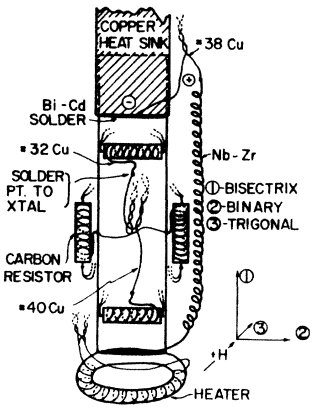

FIG. 1. The crystal holder for the measurement of the magnetoresistance, Hall effect, thermal magnetoresistance, Righi-Leduc effect, thermoelectric and Nernst-Ettinghausen effects. The orientation of the antimony single crystal relative to directions of the currents (1), of the fields measurement [(1) and (2)], and of the magnetic field (3) is also indicated.

the results of galvanomagnetic measurements at very low fields are reported. Section IVC deals with the asymptotic behavior of the various transport coefficients at high fields. Section IVD gives results and comparison with theories of the oscillations due to Landau quantization.

II. PHENOMENOLOGICAL DEFINITIONS OF THE TRANSPORT EFFECTS

All measurements were made with the magnetic field parallel to the trigonal axis with the convention indicated by Fig. 1. Threefold ($\bar{3}m$) symmetry perpendicular to the plane in which the effects are measured implies that the kinetic equations[5,6] for two-dimensional isotropic media are applicable.[24] They are

$$\text{(equipotential)} \qquad \begin{aligned} \mathbf{J} &= \hat{\sigma}\mathbf{E}^* - \hat{\epsilon}''\mathbf{G} \\ \mathbf{W}^* &= -\hat{\pi}''\mathbf{E}^* + \hat{\lambda}''\mathbf{G}. \end{aligned} \tag{1}$$

The fluxes $\mathbf{W}^*$ and $\mathbf{J}$ are the thermal and electrical current densities expressed as linear combinations of the affinities $\mathbf{G}$ (the negative of the temperature gradient) and $\mathbf{E}^*$ (the electric field). The asterisk on $\mathbf{E}^*$ and $\mathbf{W}^*$ has been used by Jan[5] to indicate that the internal quantities have been modified by a term involving the chemical potential ζ so as to represent measured quantities.[25] The kinetic coefficients defined by Eq. (1) are the quantities calculated in formal transport theories. Each is a 2×2 tensor, and by symmetry this tensor is homomorphic[26] to the complex numbers. These coefficients are named as follows: $\hat{\sigma}$, the electrical conductivity; $\hat{\lambda}''$, the thermal conductivity; $\hat{\epsilon}''$, the thermoelectric power; and $\hat{\pi}''$, the Peltier tensor $\hat{\pi}''=T\hat{\epsilon}''$. Each of these coefficients appears as a sum of the independent contributions from each carrier band plus the phonon contribution, provided band-to-band interactions and phonon drag are neglected.

The physical conditions leading to Eqs. (1) are, unfortunately, not readily attainable in the laboratory. In practice one measures the tensor $\hat{\rho}$ (electrical magnetoresistivity and Hall resistivity) defined by

$$\text{(isothermal)} \qquad \begin{aligned} \mathbf{E}^* &= \hat{\rho}\mathbf{J} + \hat{\epsilon}\mathbf{G}, \\ \mathbf{W}^* &= -\hat{\pi}\mathbf{J} + \hat{\lambda}\mathbf{G}, \end{aligned} \tag{2}$$

and obtains the quantity $\hat{\sigma}$ by a simple inversion $\hat{\sigma}=\hat{\rho}^{-1}$. The absence of primes on the other coefficients indicates the "isothermal" condition.[2] Considerable experimental and computational complexity is added if the other kinetic coefficients are to be obtained. One measures the tensors $\hat{\gamma}$ (thermal magnetoresistivity and Righi-Leduc resistivity) and $\hat{\epsilon}'$ ("adiabatic" Seebeck and Nernst-Ettinghausen effect) defined by

$$\text{"adiabatic"} \qquad \begin{aligned} \mathbf{E}^* &= \hat{\rho}'\mathbf{J} + \hat{\epsilon}'\mathbf{W}^*, \\ \mathbf{G} &= \hat{\pi}'\mathbf{J} + \hat{\gamma}\mathbf{W}^*, \end{aligned} \tag{3}$$

with the "adiabatic" condition[2] denoted by a single prime. The remaining kinetic coefficients are then obtained from the experimental coefficients through the relations $\hat{\lambda}''=\hat{\gamma}^{-1}(1+\hat{\epsilon}'^2\hat{\rho}^{-1}\hat{\gamma}^{-1}T)$ and $\hat{\pi}''=\hat{\epsilon}''T=\hat{\rho}^{-1}\hat{\epsilon}'\hat{\gamma}^{-1}T$ $=\hat{\sigma}\hat{\epsilon}'\hat{\lambda}T$. In practice, the term $\hat{\epsilon}'^2\hat{\rho}^{-1}\hat{\gamma}^{-1}T=\hat{\epsilon}'\hat{\pi}''$ is usually negligible compared to unity and it is possible to write $\hat{\lambda}''\approx\hat{\gamma}^{-1}=\hat{\lambda}$. In the present case, however, this correction was found to range from 2.5% at 1.6°K to 6.5% at 4°K. Details concerning the foundations of Eqs. (1), (2), and (3) can be found, for example, in the articles by Callen[6] and more explanation concerning their application in the present notation is in the articles by Grenier *et al.*[2,3]

III. EXPERIMENTAL DETAILS

The apparatus and measuring techniques were similar to those used in the earlier work of Grenier *et al.*,[2,3] and their description will be abbreviated accordingly.

The crystal was cut with a Servomet spark cutter from a Cominco[27] grade 69 zone-refined bar. Flat surfaces perpendicular to the trigonal axis were obtained by cleavage and the finished crystal was cleaned in an acid solution.[19] Dimensions were $20\times4.6\times2$ mm with the 4.6-mm width along a binary axis. The long dimension was held vertical and the upper end was soldered to the tip of a No. 9 copper wire (heat sink) passing from the interior of a $\frac{5}{8}$-in. cylindrical high-vacuum ($\sim4\times10^{-6}$-mm Hg) chamber containing the sample to the liquid-helium bath. The arrangement is shown to scale in Fig. 1. All solder connections were made with nonsuperconducting 60-40 Bi-Cd eutectic. The source of heat current was obtained from a 107-Ω heater which was wound from No. 40 Constantan on a hoop-shaped core of No. 16 copper wire and soldered to the lower

[24] L. Onsager, Phys. Rev. **37**, 405 (1931); **38**, 2265 (1931).

[25] J. M. Ziman, *Electrons and Phonons* (Oxford University Press, London, 1960), p. 383. The notation prime is used by Ziman in place of the asterisk.

[26] See for example C. G. Grenier, J. R. Long, J. M. Reynolds, and N. H. Zebouni, Proceedings of the 9th International Conference on Low Temperature Physics, Columbus, Ohio, 1964 (unpublished).

[27] Cominco Products, Inc., Spokane 4, Washington.

end of the crystal. Electrical current was provided by leads soldered to the upper and lower ends of the crystal. A 22-cm length of 10-mil Supercon A33 wire was used to connect the electric current lead to the heater end of the crystal. This was done in the hope that all effects could be measured without disturbing the crystal, the superconductor being able to carry high electric currents in the measurement of $\hat{\rho}$, but conducting negligible heat in the measurement of $\hat{\gamma}$ and $\hat{\epsilon}'$. This procedure was moderately successful, but some undesirable effects were observed.[28]

The difficult[23] problem of field orientation was partially solved by finding the magnetoresistance minimum[29] of a zinc crystal mounted parallel to the basal plane of the antimony.

Magnets and cryogenic equipment were identical to those used by Rao[4] with the addition of devices designed to improve the stability of the bath temperature.

For galvanomagnetic measurements, the current ranged from 1 mA for measurement of ρ_{11} at high field to 1 A for measurements at zero and low field. Heat currents for thermomagnetic measurements ranged from 0.1 mW at 1.6°K to 1.0 mW at 4°K, the main criterion in this case being to keep the temperature gradient sufficiently small (<0.1°K/cm) to apply various linear approximations in the computations.[28]

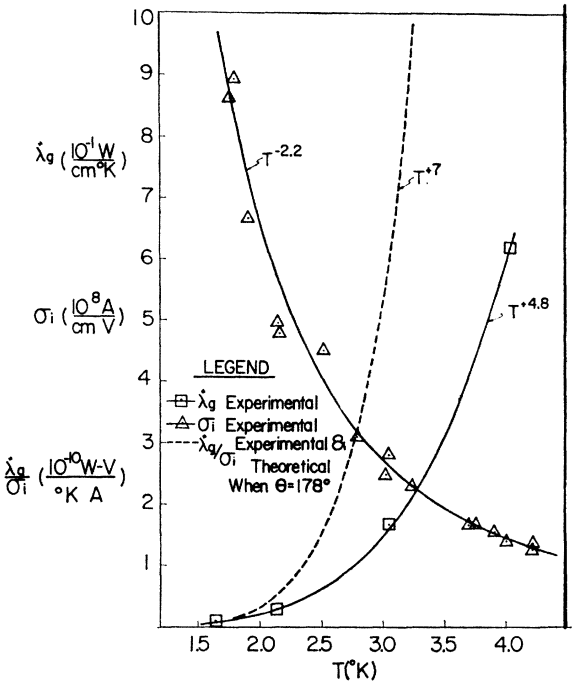

FIG. 2. The lattice thermal conductivity λ_g'' and the ideal electrical conductivity σ_i are shown as functions of temperature. The power laws of the individual conductivities do not fit the standard theory for metals (i.e., T^{+2} and T^{-5}), but the T^7 law found for the ratio λ_g''/σ_i is expected for an electron-phonon N process.

[28] J. R. Long, Ph.D. dissertation, Louisiana State University, 1965 (unpublished).

[29] P. B. Alers, Phys. Rev. **101**, 41 (1956).

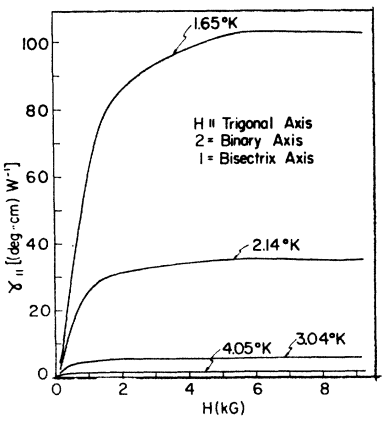

FIG. 3. The thermal magnetoresistivity γ_{11} is shown as a function of the magnetic field. It is seen to saturate to the lattice contribution at a moderate field value. The behavior of γ_{11} at higher fields is shown in Fig. 12.

IV. RESULTS AND DISCUSSION

A. The Lattice Thermal and Ideal Electrical Conductivities

1. Comparison with Standard Theories for Metals

The zero-field electrical conductivity was calculated from resistance measurements taken as a function of temperature throughout the liquid-He^4 range. The high purity and dominance of phonon scattering were demonstrated by the resistivity ratio ρ_{300}/ρ_T, which varied from 3600 at 4.2°K to 9500 at 1.2°K. When a residual resistivity $\rho_0=4\times10^{-9}\Omega$ cm was subtracted from the measured values, the resulting ideal conductivity $\sigma_{id}=(\rho_T-\rho_0)^{-1}$ was found to fit a power law $\sigma_{id}=3.07\times10^9T^{-2.2}$ A/cm V, Fig. 2. Although this is rather close to the T^{-2} law predicted for electron-electron interband scattering,[30] it will be seen that the scattering was dominated by an electron-phonon N process. The generally accepted Debye-Grüneisen-Bloch theory predicts, however, a low-temperature T^{-5} law given by[31]

$$\sigma_{e-p}=\frac{1}{4}\left(\frac{T}{\theta}\right)^{-5}\left[\mathcal{J}_5\left(\frac{\theta}{T}\right)\right]^{-1}\sigma_\theta\sim\frac{\sigma_\theta}{497.6}\left(\frac{T}{\theta}\right)^{-5} \quad (4)$$

for N-process electron-phonon scattering. $\mathcal{J}_5$ is a Debye integral, and σ_θ is the conductivity when $T=\theta$ the Debye temperature. Here there is a clear disagreement with the theory both in power law and in magnitude, the conductivity being some 1000 times larger than expected from Eq. (4).

A complementary disagreement was found in the lattice component of thermal conductivity λ_g''. It is possible to write the thermal conductivity as $\hat{\lambda}_e''+\lambda_g''\hat{1}$ where the electronic term $\hat{\lambda}_e''$ is of the form $\sim H^{-n}$ and the lattice term λ_g'' is approximately constant at a

[30] See Ref. 25, p. 416.

[31] See Ref. 25, p. 364.

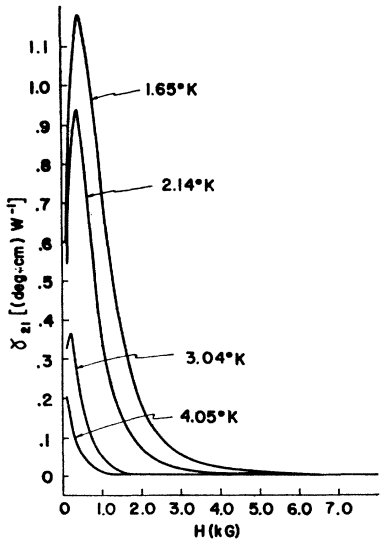

FIG. 4. The Righi-Leduc resistivity γ_{21} is shown as a function of the magnetic field. The saturation of γ_{11} at high field has the effect of making γ_{21} pass through a maximum before tending to zero at higher fields.

given temperature. Figure 3 shows that at moderately high fields the thermal resistivity γ_{11} approaches a nearly constant value which is identified as γ_g. This quenching of the electronic component of γ_{11} corresponds to the large quadratic magnetoresistance which causes the electronic term $(\lambda_{11_e}''\sim H^{-2})$ in λ_{11}'' to become negligible with respect to the lattice term. Figure 4 shows the Righi-Leduc resistivity γ_{21} approaching zero simultaneously with the saturation of γ_{11}. It follows that $\lambda_{11}=\gamma_{11}/(\gamma_{11}^2+\gamma_{21}^2)\approx 1/\gamma_{11}$, and noting that $\hat{\lambda}''=\hat{\lambda}(1+\hat{\epsilon}'\hat{\epsilon}'')\approx\hat{\lambda}$, it is concluded that the high-field measurement of γ_{11} is nearly a direct measure of $1/\lambda_g''$.

The corrected λ_g'' values are shown, in Fig. 2, as a function of temperature. It was found to obey the law $\lambda_g''=7.5\times10^{-4}T^{4.8}$ W/cm °K. Neither boundary nor isotope scattering, from which one expects a T^3 law, would result in values as small as those measured. Electrons are expected to scatter most of the phonons and for a normal process

$$\lambda_g''=\frac{27}{4\pi^2}\frac{\lambda_{e\theta}''}{n_a^2}\left(\frac{T}{\theta}\right)^2\frac{[\mathcal{J}_4(\theta/T)]^2}{\mathcal{J}_5(\theta/T)}\sim\frac{3.67}{n_a^2}\left(\frac{T}{\theta}\right)^2\lambda_{e\theta}'' \quad (5)$$

is predicted.[32] Here $\lambda_{e\theta}''$ is the zero-field electronic component of $\hat{\lambda}''$ at the Debye temperature and n_a is the number of carriers per atom which for phonon scattering purposes will be taken as the sum of the absolute values of the number of carriers per atom in each band. Electron-phonon N-scattering was expected to dominate the lattice conductivity, but the experimental result is clearly different in power law and 1000 times smaller than that predicted by Eq. (5).

These discrepancies between theoretical and measured values of σ_{id} and λ_g'' become more interesting when the ratio of the two conductivities is examined.

[32] See Ref. 25, p. 321.

From the curves which fit the experimental points, Fig. 2, it is found that

$$\lambda_g''/\sigma_{id}=2.445\times10^{-13}T^7 \text{ joule V/A °Ksec.} \quad (6)$$

When the ratio of the theoretical Eqs. (4) and (5) is taken, one obtains

$$\frac{\lambda_g''}{\sigma_{id}}=\frac{27}{\pi^2}\left[\mathcal{J}_4\left(\frac{\theta}{T}\right)\right]^2\frac{\lambda_{e\theta}''}{n_a^2\sigma_\theta}\left(\frac{T}{\theta}\right)^7=\frac{1846}{n_a^2}L_n\theta\left(\frac{T}{\theta}\right)^7, \quad (7)$$

where L_n is the theoretical Lorentz number 2.71×10^{-13} esu. Taking a consensus[7,8] value of 4×10^{19} cm^{-3} as the number of carriers in each of the (two?) bands, the value $n_a=2.42\times10^{-3}$ carriers/atom results. Equations (6) and (7) are then in perfect agreement when the characteristic temperature $\theta=178$°K is used. This value is consistent with previously reported values which have apparently ranged from 140 to 201°K.[33] Apparently most of the discussion would pertain to the right choice of n_a.[34]

As one might surmise from the agreement, the T^7 law is of a more general nature than the power laws predicted for the individual conductivities. Indeed, using a variational method, Ziman obtains[32]

$$\frac{\lambda_g''}{\sigma_{id}}\geq\frac{1}{n_a^2}\left(\frac{k}{e}\right)^2\left(\frac{C_g}{3Nk}\right)^2T, \quad (8)$$

which reduces to Eq. (7) when the Debye formula $C_g=(12\pi^4/5)Nk(T/\theta)^3$ is substituted. The inequality in Eq. (8) results when U processes which behave as $\exp(\theta/T)$ are present. The fact that an exact T^7 law is followed here means that the only scattering of any consequence is due to an electron-phonon N process.

The failure of Eqs. (4) and (5) can nevertheless be made plausible by considering the possibility that the angle of scatter in the N process is larger than T/θ, a condition which may be expected to exist for semimetals which contain small Fermi surface pockets.

2. *The Ideal Resistance of the Semimetals at Low Temperatures*

The usual criterion in a metal where an electron-phonon N process occurs is that the limiting value of the scattered-phonon wave vector q be taken as q_D, the Debye sphere radius. However, if $2k_F$, the diameter of the Fermi sphere, is smaller than q_D, the limiting value of q should be taken as $2k_F$ instead of q_D, changing Eq. (4) into

$$\sigma_{e-p}=\frac{1}{4}\left(\frac{T}{\theta^*}\right)^{-5}\left[\mathcal{J}_5\left(\frac{\theta^*}{T}\right)\right]^{-1}\sigma_\theta, \quad (9)$$

where $\theta^*=(2k_F/q_D)\theta$ is the effective Debye temperature

[33] H. M. Rosenberg, *Low Temperature Solid State Physics* (Oxford University Press, London, 1963), p. 8.

[34] If, for example, electrons and holes can be considered independent scattering centers with the same scattering efficiency, then $n_a^2\approx n_h^2+n_e^2$ and θ would be nearly 200°K.

for electron scattering. In a more usable form,

$$(\rho_T/\rho_{T'})_{e-p}=4(T/T')(T/\theta^*)^4[\mathcal{J}_5(\theta^*/T)], \quad (10)$$

where the low-temperature ideal resistivity $\rho_{T(e-p)}$ is compared with a high-temperature T' (room-temperature) resistivity. In antimony, the electron Fermi pockets are not spherical. For example, the Shoenberg ellipsoids are cigar-shaped with an almost circular cross section and a long axis about 4 times the small axis[4]:

$$(k_{1'},k_{2'},k_{3'})\simeq(4.3,3.8,17)10^6 \text{ cm}^{-1}. \quad (11)$$

At low temperatures the relaxation time depends mainly on the small cross section of the ellipsoid so that the $2k_F$ value to be used for the spherical case can be taken as the mean diameter of the ellipsoid's small cross section. With $\theta=180°$K, $q_D\simeq10^8$ cm^{-1} and $2k_F\simeq8.3\ 10^{-6}$, a value for $\theta^*=15°$K is found.

The T^5 law for resistivity would occur for $T\ll\theta^*$, but since in the present range of study, T is still of the order of θ^*, a smaller power of T dependence is to be expected in the resistivity. For example, the experimental $T^{2.2}$ law would fit closely within the range $3°<T<6°$ (i.e., $1/5<T/\theta^*<2/5$) for $\theta^*=15°$K or the range $2°<T<4°$K for $\theta^*=10°$K, whereas a $T^{2.9}$ law would be required for $2°<T<4°$K and $\theta^*=15°$K. Thus, the apparently anomalous temperature dependence, reported above, can be made plausible by these considerations.

Besides the approximate match in the temperature dependence, it is also interesting to check the order of magnitude of the effect. The experimental value for $\rho_T/\rho_{300°}$ is found to be 30 to 40 times smaller than expected from Eq. (10), and this may also be made plausible by several possible alternatives. It may be seen that an almost "full phonon drag"[48,49] could decrease the resistance by such an amount. Also the experimental $\rho_{300°}$ should correspond to a θ^* larger than its low-temperature value since the phonons involved in the scattering at room temperatures would have wave vectors larger than $2k_F$; indeed, U process, interband scattering, and scattering along the large size of the ellipsoids would not be negligible effects at room temperature. Thus the discrepancy in the resistance ratio can be taken care of by a value $\theta^*\approx37°$K at room temperature.

Another point of interest about semimetals at low temperatures as seen from Eqs. (4), (5), (8), and (9) is that the Debye T^3 law for specific heat does not impose the $\rho_{id}\sim T^5$ law nor the $\lambda_g''\sim T^2$ law which are governed by another Debye temperature, but would impose the $\lambda_g''/\sigma_{id}\sim T^7$ law which depends on the same Debye temperature.

B. Low-Field Galvanomagnetic Effects

1. Theory

One of the most complete semiclassical treatments of gross transport phenomena in a magnetic field is that of Sondheimer and Wilson.[35–37] Quantum theories yield few corrections, their effort being directed toward explaining the oscillatory effects.[38–40] Sondheimer and Wilson presented a broad treatment which, in principle, is applicable to a large variety of transport mechanisms. In the galvanomagnetic effects reported here there was probably a mixture of mechanisms due to scattering of the electron-phonon, electron-static-defect and electron-boundary types. From the mobilities, the electron mean free path was estimated to be on the order of 5% of the smallest sample dimension. (An attempt to observe magnetomorphic oscillations[41,42] of expected period ~5 G was thus unsuccessful.) Thus it was considered prudent to neglect size effects, any correction being small and hard to make.[43] The general interpolation formulas[35,36] are applicable to the problem which remains, but are so intractable as to make quantitative analysis impossible. The only manageable formulas are those that rely on integration of the Boltzmann equation by means of a relaxation time τ. These formulas (in cgs Gaussian units) are

$$H\sigma_{11}=ecH\sum_i n_i a_i H_i/(H^2+H_i^2), \quad (12a)$$

$$\sigma_{12}=ecH\sum_i(\pm)n_i/(H^2+H_i^2) \quad (12b)$$

generalized to an arbitrary number of bands. The upper and lower signs ($\pm$) denote hole and electron terms, respectively. The subscripts 1 and 2 follow the convention of Fig. 1, while e, c, and H have their usual meanings. The quantities n_i, a_i, and H_i are given for the ith band and are the carrier density, the orbital ellipticity parameter, and the saturation field, $H_i=m_i^*c/e\tau_i$, respectively.[44] The use of a relaxation time [and thus Eqs. (12)] at low temperatures is justified in principle[37] only if the scattering is of the static point-defect type (elastic). Furthermore, the condition $\omega\tau<1$ is stipulated, where $\omega=eH/m^*c$, the cyclotron frequency.

---

[35] E. H. Sondheimer and A. H. Wilson, Proc. Roy. Soc. (London) **A190**, 435 (1947).

[36] E. H. Sondheimer, Proc. Roy. Soc. (London) **A193**, 484 (1948).

[37] A. H. Wilson, *Theory of Metals* (Cambridge University Press, London, 1953), p. 193. In the semiclassical treatment, quantum statistics are applied to the classical Boltzmann equation.

[38] I. M. Lifshitz and L. M. Kosevich, Zh. Eksperim. i Teor. Fiz. **33**, 88 (1957) [English transl.: Soviet Phys.—JETP **6**, 67 (1958)].

[39] E. N. Adams and T. D. Holstein, J. Phys. Chem. Solids **10**, 254 (1959).

[40] G. E. Zil'berman, Zh. Eksperim. i Teor. Fiz. **29**, 762 (1955) [English transl.: Soviet Phys.—JETP **2**, 650 (1956)].

[41] N. H. Zebouni, R. E. Hamburg, and H. J. Mackey, Phys. Rev. Letters **11**, 260 (1963).

[42] K. R. Efferson, C. G. Grenier, and J. M. Reynolds (unpublished).

[43] See Ref. 25, p. 464.

[44] See Ref. 3. When τ is not isotropic $a=(1/2)\{R^{1/2}+R^{-1/2}\}_i$ with $R=(\alpha_{11}\tau_1)(\alpha_{22}\tau_2)^{-1}$. Subscripts 1 and 2 correspond to orientations of long and short axes of the ellipsoid's cross section by the basal plane. The tensor α is the inverse mass tensor $\hat{m}^{-1}$.

TABLE I. Two-band-model parameters as determined by fitting Eqs. (13) to $H\sigma_{11}$ and σ_{12} data as shown in Figs. 5 and 6. The results are compared with those of Rao *et al.*

	$H\sigma_{11}$					σ_{12}			
	H_h (G)	H_e (G)	$a_h n_h$ (10^{19} cm^{-3})	$a_e n_e$ (10^{19} cm^{-3})	$\frac{H_e}{H_h}$	H_h (G)	H_e (G)	$n=n_e=n_h$ (10^{19} cm^{-3})	$\frac{H_e}{H_h}$
Present work at 4°K	16.1	69.4	7.70	3.56	4.31	15.0	25	4.3	1.7
Rao *et al.* at 4.2°K	115	540	10.7	10.6	4.7	86.4	492	4.68	5.7
Present work at 1.6°K	9.88	42.3	10.23	4.74	4.28	10.0	15	4.3	1.5
Rao *et al.* at 1.7°K	101	453	11.3	12.4	4.5	79.6	459	4.93	5.8

2. *Discussion and Results*

The high purity of this crystal resulted in a dominance of phonon scattering (the zero-field data indicate that at 4°K more than 60% of the resistivity was due to phonon scattering, though at 1.6°K this figure dropped to 20%) and relaxation times so long that the value $\omega\tau=1$ was exceeded at fields below 100 G. It has been previously demonstrated that the requirement $\omega\tau<1$ is not stringent,[3,4] but the present case is a severe test. Rao *et al.*[4] applied Eqs. (12) to data from an antimony crystal in which it could be concluded from the temperature dependence of the effects that point-defect scattering was dominant. Except for the failure of the $\omega\tau<1$ condition, Eqs. (12) were valid for Rao's data. Equations (12) were also applied to data for the crystal reported here. Although phonon scattering was dominant, Eqs. (12) were found to describe the data quite well. Qualitative agreement between data at 1.6° and 4°K and a two-band fit to Eqs. (12) is shown by the curves in Figs. 5 and 6. Parameters of the two bands determined from the fits are shown in Table I where they are compared to the results of Rao *et al.*,[4] Rao's data having been corrected for an error in the measurement of the sign of the Hall effect.

The results for σ_{11} are examined first. The saturation fields are seen to be much smaller than those found by Rao, and this is the expected result of a longer relaxation time in a crystal with a lower impurity density. The temperature dependence of the H_i is likewise interpreted as due to a decreasing phonon density. The H_i appear to be decreasing to some residual value characteristic of the imperfection concentration.

The ratios H_e/H_h of the saturation fields for the two sets of data are in surprising agreement. The relaxation-time concept is apparently of broader applicability than one would expect.[37] There is no obvious reason for the relative mobilities of two bands to be the same for two completely different scattering mechanisms. It will be noticed that the agreement in the ratio H_e/H_h is somewhat better at the lowest temperatures where the scattering is more nearly comparable.

The only clear discrepancies between these σ_{11} data and those of Rao *et al.* are in the values of $n_i a_i$. The

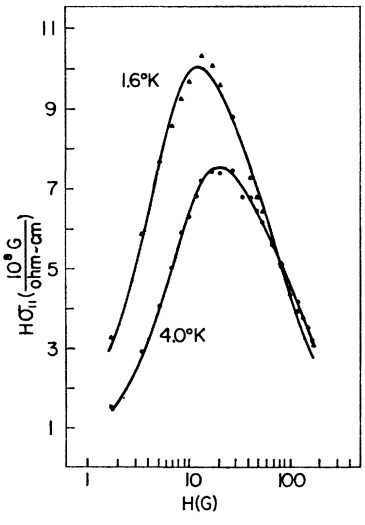

FIG. 5. The low-field electrical conductivity is shown at two temperatures as a function of the magnetic field. The maximum value of $H\sigma_{11}$ is in principle related to the carrier density, and the temperature variation is not expected from simple theories based on an isotropic relaxation time. The solid curves are least-squares fits for a two-band model and correspond to the transport parameters given in Table I.

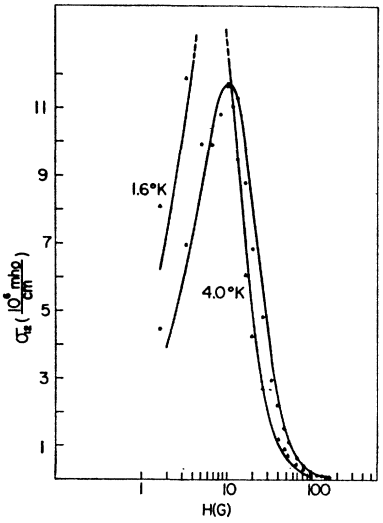

FIG. 6. The low-field Hall conductivity σ_{12} is shown as a function of the magnetic field at the temperatures of 1.6 and 4°K. For a two-band model the positive value of σ_{12} indicates that holes are more mobile than electrons. The solid curves are least-squares fits for a two-band model corresponding to the transport parameters given in Table I.

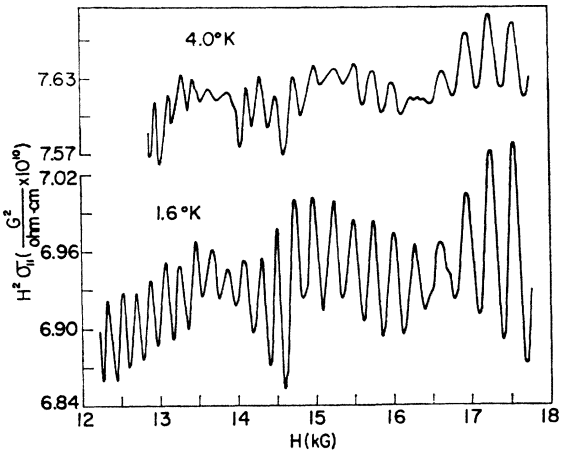

FIG. 7. The high-field behavior of the magnetoconductivity σ_{11}. The curves at 4 and 1.6°K show that the H^{-2} asymptotic behavior is well achieved. The Shubnikov–de Haas oscillations are well marked at 1.6°K; the beats are due to the misalignment of the magnetic field with the trigonal axis.

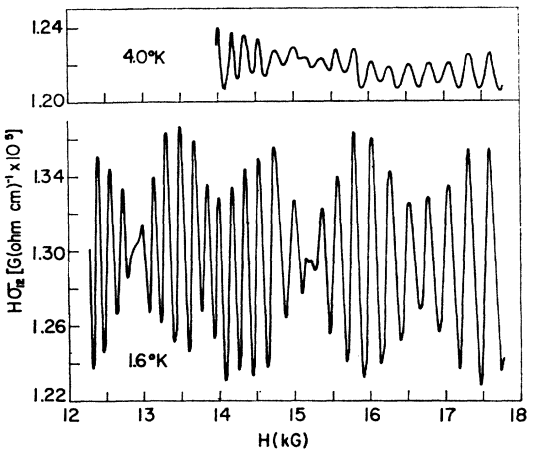

FIG. 8. The high-field Hall conductivity σ_{12} as a function of the magnetic field. The positive, nonzero asymptotic value of $H\sigma_{12}$, which is practically temperature-independent, indicates a slight excess of holes. The beats in the Shubnikov-de Haas oscillations are due to misalignment.

values obtained here are smaller than those found by Rao. With a decrease of the temperature from 4° to 1.6°K the peak of the $H\sigma_{11}$ curve, Fig. 5, is seen to rise corresponding to an increase of the $n_i a_i$ value, apparently rising toward the larger values found by Rao as the realm of static defect scattering is approached. The apparent lower values of $n_i a_i$ for the phonon-electron scattering process can be understood by noting that a longer relaxation time is expected along the longer axes of the ellipsoids than along the shorter axes, and this makes the $[\tau_j(1/m)_{jj}]_i$ ratio more isotropic than for the case of a τ_i independent of orientation. Thus a value a_i closer to unity is expected.[44]

The results of σ_{12} are not so clearly interpreted as those for σ_{11}. Qualitative agreement with a two-band model is demonstrated by Fig. 6, but the saturation fields H_e of the electron band required to fit the σ_{12} data do not agree with the results of the $H\sigma_{11}$ fittings. Satisfactory agreement was found for the band of holes. The inconsistency is best expressed through the ratio H_e/H_h which is much lower for the σ_{12} results than for the σ_{11} results. Comparison to Rao's[4] data adds confusion. In Rao's data the opposite result was found with a larger ratio H_e/H_h for σ_{12} than for σ_{11}. These discrepancies between the relative mobilities required to fit σ_{11} and σ_{12} are perhaps due to the failure of the condition $\omega\tau<1$ or some other weakness of the transport theory, but it seems also possible that the result can be explained as a failure of the two-band model.

It has been argued[7] that a three-band model should be applied to antimony. Rao *et al.*[4] showed that their Shubnikov–de Haas results were consistent with a model in which the newer[9] carriers are divided into two bands, and Datars[15] has reported three cyclotron masses in the trigonal direction. The discrepancies in the σ_{11} and σ_{12} data of Table I can be qualitatively resolved by introducing a third band of either sign and appropriate a_i values.

The number $n=4.3\times10^{19}$ cm^{-3} determined from the σ_{12} fitting is a compromise between a best fit and a reasonable value of n. An accurate determination of n cannot be made from σ_{12} when the saturation fields are not well separated. A consensus value of $n=4\times10^{19}$ cm^{-3} has been used for calculation purposes throughout this article.

C. Gross Behavior of the Kinetic Coefficients under High-Field Asymptotic Conditions

1. Galvanomagnetic Coefficients

The magnetoresistivity ρ_{11} and the Hall resistivity ρ_{21} were published earlier.[26] The field dependence of ρ_{11} was quadratic and its high field value was approximately 30 times that of ρ_{21} which exhibited a nearly cubic field dependence rather than the linear dependence expected from the assumption $n_e=n_h$.

TABLE II. Quantities determined from the high-field limiting values of the kinetic coefficients. The precision of these quantities is generally good except that associated with the quantities $f(\alpha)\Sigma_i Z_i a_i H_i$.

	4°K	3°K	2.1°K	1.6°K	Extrapolation 0°K
(Calculated from Table I)					
$10^{-21}\Sigma_i n_i a_i H_i$	3.71			3.02	
(Measured)					
$10^{-21}\Sigma_i n_i a_i H_i$	4.76	4.61	4.38	4.33	
$10^{-15}(n_h-n_e)$	7.6	8.0	7.9	8.1	
$10^{-35}f(\alpha)\Sigma_i Z_i a_i H_i$	13.0	10.5	6.72	4.84	2.4
$10^{-33}\Sigma_i Z_i$	10.9	7.48	4.45	3.05	1.52
$\alpha=L_N/L_1=\tau_\lambda/\tau_\sigma$	0.091	0.143	0.286	0.333	
$10^{-33}\alpha\Sigma_i Z_i$	1.0	1.1	1.3	1.0	

Equations (12) predict that $H^2\sigma_{11}$ and $H\sigma_{12}$ approach constant limiting values as the condition $H \gg H_i$ is attained. Figures 7 and 8 demonstrate that the gross (monotonic) part of $\hat{\sigma}$ follows this prediction. The limiting values $\sum_i n_i a_i H_i$ and $\sum_i(\pm)n_i$ are presented in Table II.

A 0.2% excess of holes over electrons is indicated by the values of $\sum_i(\pm)n_i$.

The values of $\sum_i n_i a_i H_i$ decrease with decreasing temperature as expected, but the temperature dependence is less than that predicted by the low field two-band parameters, Table I. The magnitudes of $\sum_i n_i a_i H_i$ as predicted by the low-field two-band model are included in Table II are seen to be smaller than the measured values. These features imply a tendency toward a practical equivalence of static defect and phonon scattering in high fields. The larger asymptotic values of $\sum_i n_i a_i H_i$ are also consistent with the possibility of a third band having a higher value of H_i (heavy carriers).

2. *Thermal Conductivities*

The thermal magnetoresistance γ_{11} was large and at moderate fields was so high as to cause most of the heat to be transported by the lattice (Fig. 3). The Righi-Leduc resistivity γ_{21} rose sharply to a low-field maximum and decayed to the asymptote zero at high field (Fig. 4). The latter effect is not so interesting as it appears. Because $\lambda_{11} \gg \lambda_{12}$, it follows that $\gamma_{21}=\lambda_{12}/(\lambda_{11}^2+\lambda_{12}^2) \rightarrow \lambda_{12}/\lambda_{11}^2$. At moderate fields, λ_{11} decreases as $1/H^2$ and λ_{12} decreases as $1/H$, thus causing γ_{21} to increase rapidly as H^3 until λ_{11} approaches the constant value λ_g causing γ_{21} to pass through a maximum and then decrease as $(\lambda_g^2 H)^{-1}$.

The kinetic thermal-conductivity tensor was computed and the electronic component $\hat{\lambda}_g''$ and the lattice component $\lambda_g''\hat{1}$ were separated through the relation $\hat{\lambda}''=\hat{\lambda}_e''+\lambda_g''\hat{1}$. The resulting lattice conductivity is discussed in Sec. IVA.

Band parameters of $\hat{\lambda}_e$ were not determined because low-field data were not taken and high-field asymptotic behavior did not occur until fields in which an accurate determination of $\hat{\lambda}_e$ was ruled out by the dominance of $\lambda_g\hat{1}$. The onset of asymptotic behavior did not occur at the low fields observed in the galvanomagnetic measurements. Because phonon scattering is more efficient in a thermal process than in an electrical process, the behavior of the thermal effects is characterized by higher saturation fields $H_{i\lambda}$ than the fields $H_{i\sigma}$ found in an electrical measurement.

3. *Lorentz Numbers and the Scattering Efficiency*

It is customary in studies where the electrical and thermal conductivities have been measured to compare the results with the Wiedemann-Franz law $\hat{\lambda}''=L_n T\hat{\sigma}$. The Wiedemann-Franz law is applicable, however, only to the conductivity that results after any significant contribution by the lattice has been subtracted, and then only when the scattering is such (at helium temperatures, static defect scattering) that both thermal and electrical processes can be characterized by the same relaxation time. If the scattering is inelastic (phonons) a small-angle scatter in energy through the Fermi surface may be as efficient in restoring thermal equilibrium as an angle π in the electrical process.[45]

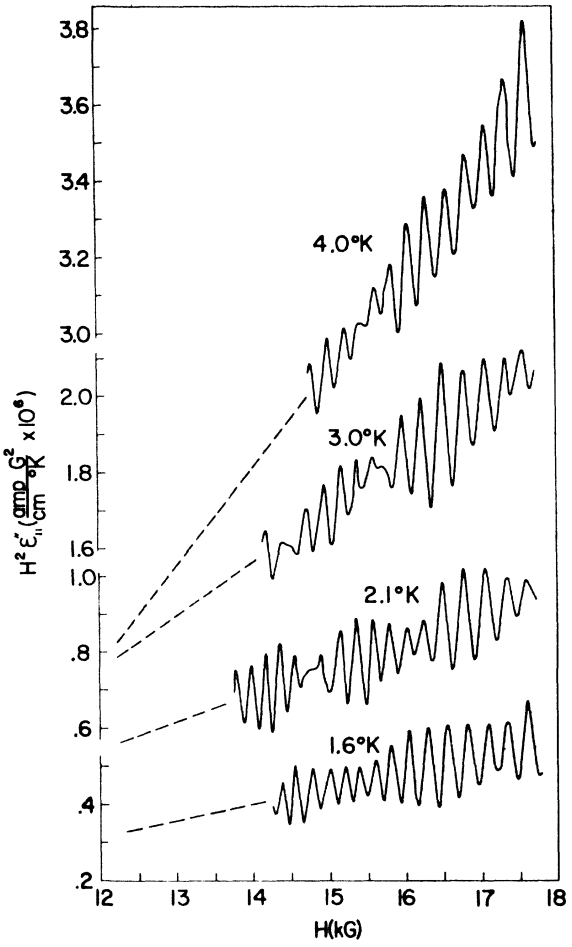

FIG. 9. The high-field thermoelectric kinetic coefficient ϵ_{11}'' as a function of the field. The positive effect is characteristic of an electron-majority type of thermoelectric effect. The field dependence is anomalous in departing clearly from the expected H^{-2} behavior. The oscillations probably arise from the scattering mechanism developed in Zil'berman's theory.

In order to adapt the Wiedemann-Franz law to phonon scattering, a thermal relaxation time τ_λ and an electrical relaxation time τ_σ were postulated[46] where

$$\tau_\lambda=\alpha\tau_\sigma; \quad \alpha \leq 1,$$

the "efficiency" α becoming unity when the scattering is strictly elastic.

[45] See Ref. 25, p. 386.

[46] K. Bordoloi, Ph.D. dissertation, Louisiana State University, 1964 (unpublished).

The efficiency may be determined from the measured Lorentz numbers defined by $L_1=\lambda_{11e}''/\sigma_{11}T$ and $L_2=\lambda_{12}''/\sigma_{12}T$ where $\hat{\lambda}''=\hat{\lambda}_e''+\lambda_g''\hat{1}$. When $\alpha=1$, $L_1=L_2=L_n$. Because the relaxation time appears only in $H_i=m_i^*c/e\tau$, the role of α is to replace $H_{i\sigma}$ by $H_{i\lambda}=(1/\alpha)H_{i\sigma}$ in the expressions for $\hat{\lambda}_e''$ derived by combining Eqs. (12) and the relation $\hat{\lambda}_e''=L_nT\hat{\sigma}$. Only in the extremes of low and high field does L_n have a simple relationship to L_1 and L_2, namely

$$\lim H_{\to 0}L_1=\alpha L_n, \quad \lim H_{\to\infty}L_1=(1/\alpha)L_n, \tag{13a}$$

$$\lim H_{\to 0}L_2=\alpha^2 L_n, \quad \lim H_{\to\infty}L_2=L_n. \tag{13b}$$

Thermal data were not taken at fields sufficiently low for the lower limits to apply and it was difficult to obtain satisfactory high-field results because of the dominant lattice conductivity. Values of α obtained from the relation $L_1=(1/\alpha)L_n$ are given in Table II. An empirical proportionality between α and the effective density of states is noted without further comment. Division of the H_i in Table I by the appropriate α should provide estimates of the band parameters for $\hat{\lambda}_e$. The increase in α from $\sim 1/10$ at 4°K to $\sim 1/3$ at 1.6°K corresponds to the increasing percentage of boundary and impurity scattering ($\alpha=1$) found in the $\hat{\sigma}$ results discussed earlier. Were the impurities not present, α should tend to zero at zero degrees in a bulk specimen.

In a study of the Lorentz numbers of tin, Bordoloi[46] found very good agreement with the complete set of Eqs. (13) thus lending more weight to the relaxation-time concept. These limited results on antimony support those findings.

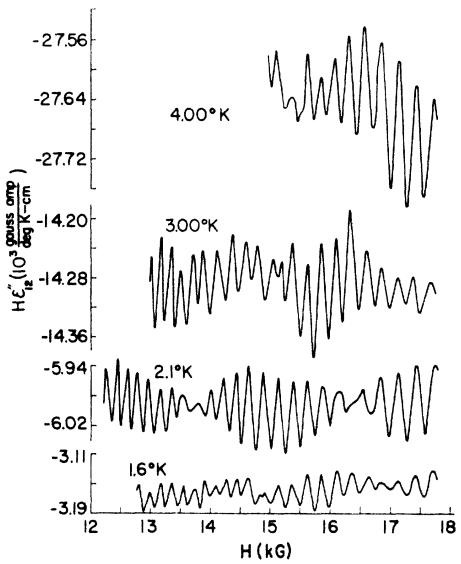

FIG. 10. The high-field Nernst-Ettinghausen kinetic coefficient ϵ_{12}'' as a function of the field. The H^{-1} asymptotic dependence is well illustrated. The values of $H\bar{\epsilon}_{12}''$ at the different temperatures are used for the determination of the density of state Z^{eff} shown in Fig. 11. The oscillations are probably due to oscillations in the density of states as a function of the magnetic field.

4. *Thermoelectric Coefficients*

The experimental thermoelectric tensor $\hat{\epsilon}'$ was reported earlier.[26] The Seebeck coefficient ϵ_{11}' exhibited a complicated behavior at moderate fields of the same nature as that observed in γ_{21}. The high-field dependence of ϵ_{11}' was approximately $\sim H^{2.5}$ with a negative value, whereas a quadratic dependence was expected. The Nernst-Ettinghausen coefficient ϵ_{21}' was positive and slightly quadratic at the lowest fields, but exactly linear above 500 G as expected.

In computing the kinetic tensor $\hat{\epsilon}''$, no correction was made for the effect of the Constantan leads. Effects due to the neglect of ϵ_{cn} were estimated to be on the order of those due to copper[2,3] and hence negligible at all but the lowest fields.

Integration of the Boltzmann equation by means of a relaxation time resulted in Eqs. (12). The same theory,[36,37] when used to calculate a heat current density, results in the equations

$$H\epsilon_{11}''=-\tfrac{1}{3}\pi^2k^2cTH\sum_i(\pm)\frac{a_if(\alpha)H_iZ_i}{H^2+[f(\alpha)H_i]^2}, \tag{14a}$$

$$\epsilon_{12}''=-\tfrac{1}{3}\pi^2k^2cTH\sum_i\frac{Z_i}{H^2+[f(\alpha)H_i]^2} \tag{14b}$$

for the kinetic Seebeck and Nernst-Ettinghausen coefficients. The notations and conventions are those used for Eqs. (12) with the addition of the densities of states Z_i and an undetermined empirical function f of the scattering efficiency α. In view of the success of Eqs. (12) in describing the galvanomagnetic effects, a fit of Eqs. (14) to $\hat{\epsilon}''$ should be attempted, but the necessary low-field data are not available for this article.

Figures 9 and 10 show the high-field quantities $H^2\epsilon_{11}''$ and $H\epsilon_{12}''$. Equations (14) indicate that these quantities should become constant at high field. It is evident from Fig. 10 that $\bar{\epsilon}_{12}''$ has the expected $1/H$ asymptotic dependence. The sums of the densities of states $\sum_iZ_i$ resulting from the high-field values of $H\bar{\epsilon}_{12}''$ are given by Table II. The $\sum_iZ_i$ are much larger than the estimated value of 0.8×10^{33} erg^{-1} cm^{-3} obtained with quadratic bands.[47] The large temperature dependence of $\sum_iZ_i$ is also unexpected, but will be seen to be related to a phonon-drag effect.[48,49]

[47] Taking only two bands, Rao's (Ref. 4) value $\zeta=1.3\times10^{-13}$ erg will be assumed for the new carriers (Ref. 9) and a consensus of $\zeta=1.9\times10^{-13}$ erg supported by the temperature dependence of our Shubnikov–de Haas oscillations will be used for the tilted ellipsoids (Ref. 8). With $n=4\times10^{19}$ cm^{-3}, an estimate $\Sigma_iZ_i=(3/2)\Sigma_in_i/\zeta_i=0.8\times10^{33}$ erg^{-1} cm^{-3} is obtained and is seen to be much less than the values obtained from ϵ_{12}''.

[48] See, for instance, D. K. C. MacDonald, *Thermoelectricity* (John Wiley & Son, Inc., New York, 1962), p. 92.

[49] See, for instance, J. M. Ziman, *Principles of the Theory of Solids* (Cambridge University Press, London, 1964), pp. 209 and 410.

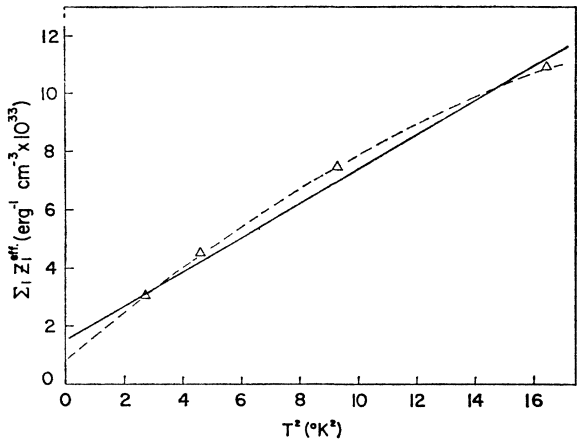

FIG. 11. The values of the apparent density of states Z^{eff} obtained from the asymptotic high-field $H\epsilon_{12}''$ quantities are plotted as functions of T^2. The T^2 dependence, as outlined by the solid straight line, is in close agreement with the influence of phonon drag on the Nernst-Ettingshausen kinetic coefficient.

The gross term in ϵ_{11}'' does not have the $1/H^2$ high-field dependence expected from Eqs. (14), but instead the equivalent of a $1/H$ dependence is found as evidenced by the linear behavior of the $H^2\epsilon_{11}''$ plot (Fig. 9). This unexplained field dependence may be a phonon-drag effect, but the unhappy possibility that the Constantan leads were responsible will have to be investigated.

5. *Phonon Drag*

The theory of phonon drag takes its simplest form when the lattice thermal resistivity is due to electron-phonon N scattering,[48,49] as found in this crystal. In a naïve way, it may be said that the electrons carry not only their own specific heat C_e, but also part or all of the specific heat of the phonons which they drag along, i.e., $\frac{1}{3}C_g$ (the $\frac{1}{3}$ corresponding to the fact that only the longitudinal phonons are involved in the N process). This should greatly affect the thermoelectric tensor coefficient. The simplest relation between the specific heat and these coefficients is that for the asymptotic value of the kinetic Nernst-Ettingshausen coefficient

$$\epsilon_{12}''=\frac{-c}{H}C_e=\frac{-\pi^2k^2cT}{3H}Z_e, \qquad (15)$$

where C_e and Z_e are, respectively, the specific heat and density of states of the electrons. The high-field ϵ_{12}'' as well as the specific heat C_e are, as seen from Eq. (15), valuable for the determination of the density of states, but should a "full phonon drag" induce an apparent specific heat $C_e+\frac{1}{3}C_g$, then an effective density of states Z^{eff} would be determined from the experimental ϵ_{12}'' data such that

$$Z^{eff}=Z_e+\frac{12}{5}\frac{N}{k\theta}\left(\frac{T}{\theta}\right)^2.$$

With the $Z_e=\sum_i\frac{3}{2}(n_i/\zeta_i)$ determined from Rao's[47] data and θ taken as 180°K, the expected behavior of the "full phonon drag" effective density of states is given by

$$Z^{eff}=(0.8+0.5T^2)10^{33}\ \text{erg}^{-1}\ \text{cm}^{-3}.$$

The same quantity determined from the experimental high-field ϵ_{12}'' data would be given by

$$Z^{eff}=(1.5+0.59T^2)10^{33}\ \text{erg}^{-1}\ \text{cm}^{-3}.$$

This behavior is illustrated in Fig. 11 where the experimental quantities Z^{eff} are plotted versus T^2. The agreement in the drag term can be considered as excellent in view of the crudeness of the approximation. The extrapolated density of states is reasonable although still about twice the theoretical value.

It is interesting to note that the exact theoretical intercept can be obtained with a smooth curve passing through each data point. One might thus speculate that an increasing fraction of electron-impurity scattering with decreasing temperature would so modify the drag term, but the accuracy of the data does not warrant placing any weight on such an extension. A better free-electron intercept would also be obtained by ignoring the point at 4°K on the grounds that this point was modified by the last vestiges of the U process. On the other hand, those who advocate a three-band model may welcome the high density of states as evidence of a band of heavy carriers.[7]

The high density of states calculated from $\hat{\epsilon}''$ measurements[3] for bismuth should possibly also be attributed to phonon drag, but the interpretation is unclear because $\hat{\epsilon}''$ was not significantly temperature-dependent in bismuth.[50] It has been suggested[51] that because of the possibility of "saturation" effects, the absence of temperature dependence in $\hat{\epsilon}''$ should not rule out the presence of a large phonon-drag contribution to $\sum_i Z_i^{eff}$. These results may also throw some light on the high densities of states obtained from specific-heat measurements reported for antimony[52] and bismuth.[53]

D. Oscillations in the Transport Coefficients

1. *Descriptive*

Oscillations due to Landau quantization with the trigonal axis period $\Delta(1/H)=10.1\times10^{-7}$ G^{-1} of the Shoenberg[8] tilted ellipsoids were found in all of the transport coefficients except γ_{21} and the corresponding λ_{12}''. Faint oscillations were observed in γ_{21}, but were discounted as a spurious effect due to probe misalignment or the Peltier heat of phonon drag.

[50] J. R. Sybert, Ph.D. dissertation, Louisiana State University, 1962 (unpublished).
[51] R. T. Delves (private communication).
[52] See, for instance, C. Nanney, Ref. 19. This is one of several papers quoting the unpublished results of N. M. Walcott.
[53] I. N. Kalinkina and P. G. Strelkov, Zh. Eksperim. i Teor. Fiz. 34, 616 (1958) [English transl.: Soviet Phys.—JETP 7, 426 (1958)].

The oscillations, Figs. 7–10, in the galvanomagnetic and thermoelectric coefficients are shown in terms of the quantities $H^2\sigma_{11}$, $H\sigma_{12}$, etc., which should become constant for the gross component of the effects under asymptotic ($H \gg H_i$) conditions, Eqs. (12) and (14). The oscillations contain beats and other irregularities in the amplitude. The three ellipsoid periods do not degenerate into a single period unless the field is oriented well within 1° of the trigonal axis, and it was not possible to obtain such precise alignment with the rigid calorimetric apparatus. There are also some slight change of orientation between different sets of measurement which add to the confusion. Antimony is thus not an ideal subject for the measurement of oscillation amplitudes and quantitative comparison with theory, though in the present state of the theory this should cause little concern.

In every effect, the oscillations were almost perfectly sinusoidal and almost without harmonics, although some second harmonic could be seen in ρ_{21} during the beats.

2. *The State of the Theory*

A quantitative theory as satisfactory as that of the de Haas–van Alphen effect has not been developed for the transport effects. Because of the complications of scattering, the effects cannot be explained directly in terms of the grand canonical potential as is done for the susceptibility.[54] Present theories fall into two categories: those that treat the oscillations as due to fluctuation in the carrier density,[38] and those that obtain oscillations as a result of the effect that quantization has on scattering.[39,40,55,56] In every case, the oscillations (denoted by symbols with tildes) have been treated as a modulation of the gross effect (bars). Thus, the total transport coefficient is, for example, written $\sigma_{11}=\bar{\sigma}_{11}+\tilde{\sigma}_{11}$.

Three independent mechanisms have been treated: (1) Zil'berman[40] considered scattering between states of the Landau level closest to the Fermi surface and states of other occupied levels. Using a distribution function, $\tilde{\sigma}_{11}$ and $\tilde{\epsilon}_{11}''$ were calculated. (2) Working through the grand canonical potential, Lifshitz and Kosevich[38] (LK) attempted to extend their susceptibility theory to the transport effects. Formulas for $\tilde{\sigma}_{11}$ and $\tilde{\sigma}_{12}$ were obtained, with oscillations arising from $\tilde{n}$, an oscillation in the carrier density at the Fermi surface. (3) Adams and Holstein[39] (AH) applied the density matrix method to Zil'berman's mechanism and, in addition, obtained a second term representing the scattering between states entirely within the level lying closest to the Fermi surface. Only $\tilde{\sigma}_{11}$ was calculated.

It should be pointed out that a choice between these theories is unnecessary. As each mechanism is, to a great extent, independent of the others, their results are superposable within a phase. Of these results, the second AH term was neglected in the comparison of the theories to the data. Although the second AH term can be very large at high fields and extremely low temperatures, a simple calculation[46] from the AH formulas showed the second AH term to be insignificant in comparison to the Zil'berman term for the fields and temperatures of the present work. A visual inspection of the sinusoidal nature of the oscillations gives, in fact, a clear indication that the second AH term should not be considered.

A useful extension was made by Horton[56] which applied the density matrix formalism to the Zil'berman scattering and extended it to find expressions for $\tilde{\sigma}_{12}$ and $\tilde{\epsilon}_{12}''$. There is also an important oscillatory term in $\hat{\epsilon}''$ which simply arises by substituting an oscillatory density-of-states term (DS), obtained by differentiating the phase of Eq. (14), into the classical equations, Eq. (11).[2,3]

Measured amplitudes of the oscillations reported here were compared with the amplitudes predicted by the Zil'berman and Horton (ZH) theories and with the LK and DS results where applicable. An additional summary of quantum transport theories in the present notation may be found in the articles by Grenier *et al.*[2–4]

3. *Oscillations in the Conductivity* $\hat{\sigma}$

Measured values of relative and absolute amplitudes of $\tilde{\sigma}_{11}$ and $\tilde{\sigma}_{12}$ for several temperatures and fields are compared in Table III with LK and ZH amplitudes.

The complicated LK formulas take a rather simple form in the case of two compensated bands.[4] The three-ellipsoid LK contribution to be expected in antimony when all bands are asymptotic is

$$|\tilde{\sigma}_{\alpha\beta}| = \bar{\sigma}_{\alpha\beta}\frac{\zeta^T}{\zeta^T+\zeta^W}\left|\frac{\tilde{n}}{n}\right|, \tag{16}$$

where $\bar{\sigma}_{\alpha\beta}$ is the measured gross component of $\sigma_{\alpha\beta}$ and the superscripts on the chemical potential ζ denote the bands corresponding to Shoenberg's[8] tilted (T) and Saito's[9] warped (W) ellipsoids. The relative amplitude of the fundamental oscillation in carrier density is

$$\frac{\tilde{n}}{n} = (\tfrac{3}{2}\pi)(\tfrac{1}{2}P_TH)^{3/2}\frac{\Lambda_T}{\sinh\Lambda_T}\cos\frac{\pi m^*}{m_0}\cos\left(\frac{2\pi}{P_TH}+\varphi\right), \tag{17}$$

where P_T is the period $\Delta(1/H)$ of the oscillation and $\Lambda_T=(2\pi^2kT)/(\zeta^TP_TH)$ is the temperature factor. The effect of the splitting factor $\cos\pi m^*/m_0\sim 0.96$ is small.

The ZH formulas used are not strictly applicable, as they were derived only for a spherical energy surface. The ZH amplitude is expressed in terms of the contribu-

[54] I. M. Lifshitz and A. M. Kosevich, Zh. Eksperim. i Teor. Fiz. **29**, 730 (1955) [English transl.: Soviet Phys.—JETP **2**, 636 (1956)].
[55] V. G. Skobov, Zh. Eksperim. i Teor. Fiz. **38**, 1304 (1960) [English transl.: Soviet Phys.—JETP **11**, 941 (1960)].
[56] P. B. Horton, Ph.D. dissertation, Louisiana State University, 1964 (unpublished).

TABLE III. Measured amplitudes of oscillations in the components $\sigma_{\alpha\beta}$ of $\hat{\sigma}$ as a percentage $|\sigma_{\alpha\beta}|/\bar{\sigma}_{\alpha\beta}\times 100\%$ of the monotonic gross effect and measured absolute amplitudes $|\sigma_{\alpha\beta}|$. Comparison to absolute amplitudes predicted by Lifshitz-Kosevich (LK) and Zil'berman-Horton (ZH) theories. LK amplitudes were computed from Eqs. (16) and (17) using the measured gross conductivities for $\bar{\sigma}_{\alpha\beta}$. ZH amplitudes were computed from Eqs. (18) using the curve-fit parameters, Table I, of the electron band to compute the contributions $\bar{\sigma}_{\alpha\beta}{}^{T}$ to the gross conductivities from the tilted ellipsoids. Data are for three approximate beat-maximum field values at each of four temperatures.

	$\frac{\lvert\tilde{\sigma}_{11}\rvert}{\bar{\sigma}_{11}}$ Meas. (%)	$\lvert\tilde{\sigma}_{11}\rvert$ Meas. $\left(\frac{\text{mho}}{\text{cm}}\right)$	$\lvert\tilde{\sigma}_{11}\rvert$ LK $\left(\frac{\text{mho}}{\text{cm}}\right)$	$\lvert\tilde{\sigma}_{11}\rvert$ ZH $\left(\frac{\text{mho}}{\text{cm}}\right)$	$\frac{\lvert\tilde{\sigma}_{12}\rvert}{\bar{\sigma}_{12}}$ Meas. (%)	$\lvert\tilde{\sigma}_{12}\rvert$ Meas. $\left(\frac{\text{mho}}{\text{cm}}\right)$	$\lvert\tilde{\sigma}_{12}\rvert$ LK $\left(\frac{\text{mho}}{\text{cm}}\right)$	$\lvert\tilde{\sigma}_{12}\rvert$ ZH $\left(\frac{\text{mho}}{\text{cm}}\right)$	H Approx. meas. (kG)
	0.5	1.9	0.36	34	4.4	0.43	0.009	0.092	13
1.6°K	0.6	1 6	0.38	29	5.1	0.38	0.011	0.065	16
	1.2	2.7	0.38	27	4.5	0.33	0.012	0.053	17.6
	0.5	1.9	0.27	26	2.0	0.20	0.006	0.088	13
2 1°K	0.7	2.0	0.31	24	1.9	0.16	0.009	0.067	16
	1.3	2.8	0.31	23	1.8	0.13	0.010	0.057	17.6
	0.3	1.4	0.14	14			0.003	0.068	13
3.0°K	0.5	1.4	0.20	16	1.8	0.15	0.006	0.062	16
	0.8	1.9	0.24	16			0.007	0.056	17.6
	0.3	1.5	0.08	7			0.002	0.043	13
4.0°K	0.2	0.5	0.12	9	0.6	0.05	0.003	0.048	16
	0.4	1.0	0.15	10	0.9	0.06	0.004	0.048	17.6

tion $\bar{\sigma}_{\alpha\beta}{}^{T}$ to the gross effect by the band which gives the oscillations, namely,

$$\tilde{\sigma}_{11}=\bar{\sigma}_{\alpha\beta}{}^{T}\frac{5\sqrt{2}}{4}(P_TH)^{1/2}\frac{\Lambda_T}{\sinh\Lambda_T}\cos\left(\frac{2\pi}{P_TH}-\frac{5\pi}{4}\right), \tag{18a}$$

$$\tilde{\sigma}_{12}=\bar{\sigma}_{12}{}^{T}\frac{7\sqrt{2}}{4}\left(\frac{H_T}{H}\right)^{2}(P_TH)^{1/2}\frac{\Lambda_T}{\sinh\Lambda_T}\cos\left(\frac{2\pi}{P_TH}-\frac{\pi}{4}\right). \tag{18b}$$

In the present approximation, the LK and ZH equations differ mainly in their field dependence.

The results for $\tilde{\sigma}_{11}$ differ somewhat from those of Rao *et al.*[4] who obtained rather good agreement between Zil'berman's $\tilde{\sigma}_{11}$ formula and their data, but found the LK predictions for $|\tilde{\sigma}_{11}|$ to be roughly only 1/40 of their measurement. The LK $|\tilde{\sigma}_{11}|$ predictions are up to about 1/10 of the present results, while the Zil'berman results are about 10 times the experimental values. These differences may be consequences of phonon scattering in this crystal as opposed to impurity scattering for Rao, although theoretical considerations[39] indicate about equal amplitudes for the two types of scattering.

Both LK and ZH underestimate the amplitudes of $\tilde{\sigma}_{12}$, though the ZH predictions are rather close at the higher temperatures. The LK values are 15 to 40 times too small.

The relative phase of the oscillations bears mentioning. Whereas $\tilde{\sigma}_{11}$ and $\tilde{\sigma}_{12}$ should be in phase according to LK and out of phase according to ZH, the measured conductivities differed in phase by slightly less than $\frac{1}{2}\pi$.

4. Oscillations in the Thermoelectric Tensor $\tilde{\epsilon}''$

Measured values of relative and absolute amplitudes of $|\tilde{\epsilon}_{11}''|$ and $|\tilde{\epsilon}_{12}''|$ for several temperatures and fields are compared in Table IV with DS and ZH amplitudes.

In the ZH formulas, Horton's expression for $\tilde{\epsilon}_{12}$ has been modified by the empirical function f of the scattering α with the result

$$\tilde{\epsilon}_{11}''=\tilde{\epsilon}_{11}''{}^{T}\frac{15\pi\sqrt{2}}{4}(P_TH)^{-1/2}\times\left[\frac{1-\Lambda_T\coth\Lambda_T}{\Lambda_T\sinh\Lambda_T}\right]\cos\left(\frac{2\pi}{P_TH}+\frac{\pi}{4}\right), \tag{19a}$$

$$\tilde{\epsilon}_{12}''=\tilde{\epsilon}_{12}''{}^{T}\frac{21\pi\sqrt{2}}{5}(P_TH)^{-1/2}\left(\frac{f(\alpha)H_T}{H}\right)^{2}\times\left[\frac{1-\Lambda_T\coth\Lambda_T}{\Lambda_T\sinh\Delta_T}\right]\cos\left(\frac{2\pi}{P_TH}-\frac{3\pi}{4}\right). \tag{19b}$$

Again it is noted that the expressions are only strictly applicable to a spherical band. In computations of the gross effect contribution from the tilted ellipsoids, it was necessary to make some assumption as to which band the tilted ellipsoids should be assigned. The usual[14,16] electron assignment was made, though with some misgiving.

The DS oscillations originate in the derivative $\partial\tilde{n}/\partial\zeta^{T}$ of the factor $\cos(2\pi/P_TH)$ in Eq. (17) with the result

$$\tilde{Z}_T=2\pi(m^*c/e\hbar H)\tilde{n}, \tag{20}$$

TABLE IV. Measured amplitudes of oscillations in the components $\epsilon_{\alpha\beta}''$ of ϵ'' as a percentage $|\epsilon_{\alpha\beta}''|/\epsilon_{\alpha\beta}''\times 100\%$ of the monotonic gross effect and measured absolute amplitudes $|\tilde{\epsilon}_{\alpha\beta}''|$. Comparison to absolute amplitudes predicted by density of states (DS) oscillations, and Zil'berman-Horton (ZH) theory. DS amplitudes were calculated from Eqs. (17), (20), and (21). ZH amplitudes were computed from Eq. (19) using parameters of the electron band, Table I, to calculate the gross-effect contributions $\tilde{\epsilon}_{\alpha\beta}{}^T$ of the tilted ellipsoids. These numbers are only of order-of-magnitude accuracy because the band parameters entering the thermoelectric effects, having not been measured, could only be estimated. For $f(\alpha)$ the purely arbitrary function $[(1+\alpha^2)/2]^{-1/2}$ was assumed. The left-column ZH values at each point were calculated from a fraction $\zeta^W/(\zeta^T-\zeta^W)$ of the measured (including drag) density of states while the right-column values in parentheses were computed using the theoretical value $\frac{3}{2}(n/\zeta^T)$.

	$\frac{\lvert\tilde{\epsilon}_{11}''\rvert}{\tilde{\epsilon}_{11}''}$	$\lvert\tilde{\epsilon}_{11}''\rvert$	$\lvert\tilde{\epsilon}_{11}''\rvert$	$\lvert\tilde{\epsilon}_{11}''\rvert$	$\frac{\lvert\tilde{\epsilon}_{12}''\rvert}{\tilde{\epsilon}_{12}''\rvert}$	$\lvert\tilde{\epsilon}_{12}''\rvert$	$\lvert\tilde{\epsilon}_{12}''\rvert$	$\lvert\tilde{\epsilon}_{12}''\rvert$	H
	Meas. (%)	Meas. $\left(\frac{10^{-4}\text{A}}{\text{cm°K}}\right)$	DS $\left(\frac{10^{-4}\text{A}}{\text{cm°K}}\right)$	ZH $\left(\frac{10^{-4}\text{A}}{\text{cm°K}}\right)$	Meas. (%)	Meas. $\left(\frac{10^{-4}\text{A}}{\text{cm°K}}\right)$	DS $\left(\frac{10^{-4}\text{A}}{\text{cm°K}}\right)$	ZH $\left(\frac{10^{-4}\text{A}}{\text{cm°K}}\right)$	Approx. meas. (kG)
			0.62	180 (46)	0.5	13	120	0.53 (0.14)	13
1.6°K	20	3.9	0.53	132 (34)	0.8	16	126	0.33 (0.08)	16
	19	3.4	0.48	112 (28)	0.6	11	126	0.24 (0.06)	17.6
			0.67	260 (46)	0.6	29	118	0.91 (0.16)	13
2.1°K	15	4.8	0.60	214 (38)	0.8	29	131	0.64 (0.11)	16
			0.57	187 (33)	0.8	27	136	0.48 (0.08)	17.6
			0.57	310 (33)	0.4	47	89	1.5 (0.16)	13
3.0°K	10	7.0	0.61	313 (33)	0.4	41	118	1.3 (0.13)	16
			0.61	298 (30)			130	1.1 (0.11)	17.6
			0.40	229 (16)			60	1.5 (0.11)	13
4.0°K	4.5	5.5	0.50	300 (21)	0.1	25	92	1.7 (0.12)	16
	5.8	6.8	0.53	309 (22)	0.2	40	108	1.6 (0.11)	17.6

valid for a Fermi sphere with $P_T=e\hbar/m^*c\zeta^T$. The classical Eqs. (14) will then oscillate according to the relation

$$\tilde{\epsilon}_{\alpha\beta}{}''^T=\tilde{\epsilon}_{\alpha\beta}{}''^T\tilde{Z}_T/\bar{Z}_T. \tag{21}$$

The use of Eq. (21) is not rigorously justified, but gives some insight, at least, into the role that the carrier's density-of-states fluctuation plays in the thermopowers.

The DS theory underestimates $|\tilde{\epsilon}_{11}''|$ (by about a factor 10) as should be expected for a longitudinal effect sensitive mainly to scattering. The ZH theory predicts a result 3 to 8 times that measured for $|\tilde{\epsilon}_{11}''|$.

The converse was found for $\tilde{\epsilon}_{12}''$ with the DS theory giving oscillations 3 to 10 times those measured and the ZH theory predicting less than 1% of the measured effect. As the transverse effects are not very scattering-sensitive at high field, the ZH theory should be expected to give a low result.

The phase between $\tilde{\epsilon}_{11}''$ and $\tilde{\epsilon}_{12}''$ was found to be approximately $5\pi/8$, with the $\tilde{\epsilon}_{11}''$ oscillation almost exactly in phase with $\tilde{\sigma}_{12}$. The ZH theory predicts a difference of π between $\tilde{\epsilon}_{11}''$ and $\tilde{\epsilon}_{12}''$.

Oscillatory transport theories usually fail by predicting a result less than the measured effect. The present situation, with overestimates for $\tilde{\sigma}_{11}$ and $\tilde{\epsilon}_{11}''$ by ZH and for $\tilde{\epsilon}_{12}''$ by DS is unusual.[2,3] The possibility that the predictions could be reduced by collision broadening may be considered. In the DS theory, for instance, Eq. (21) might be multiplied by a broadening term $\exp(2\pi/\omega\tau_c)$ as used by Adams and Holstein,[39] where ω is the cyclotron frequency and τ_c is a cutoff time expected to be comparable in magnitude to the relaxation time τ. But in order to resolve the difference between the measured and DS values of $|\tilde{\epsilon}_{12}''|$ by such a term, however, cutoff times of order 10^{-12} sec would be required, whereas the relaxation times calculated from the saturation fields of the low-field galvanomagnetic effects are of order 10^{-10} sec.

5. *Oscillations in the Lattice Conductivity*

Oscillations in the lattice thermal resistivity γ_{11}, Fig. 12, were not of the usual type that arise by an application of the Wiedemann-Franz law to σ. It was previously observed that in fields greater than a few kilogauss, $\gamma_{11}{}^{-1}\approx\lambda_g''$. In accordance with this observation, the oscillations in γ_{11} will be shown to be the result of oscillations in the lattice conductivity.

The oscillations in γ_{11} are in phase with $\tilde{\sigma}_{11}$ and have the period and typical beats of the Shoenberg[8] ellipsoids. The temperature dependence of the amplitude is exceptionally large.

As it was known that scattering by electrons limited the gross lattice conductivity, Fig. 2, it seemed likely, upon observing the effect, that the oscillations were due to the fluctuation in the number of scattering centers. Several other possible origins were considered, however.

The Wiedemann-Franz law is always at least qualitatively applicable in a metal. Thus, if σ_{11} oscillates, it is normal to find oscillations in the electronic component of the thermal conductivity with an amplitude under asymptotic conditions given by $|\tilde{\lambda}_{11}''|=(1/\alpha)\times L_nT|\tilde{\sigma}_{11}|$. When the measured values of $|\tilde{\sigma}_{11}|$ were substituted into this relation, a number of order

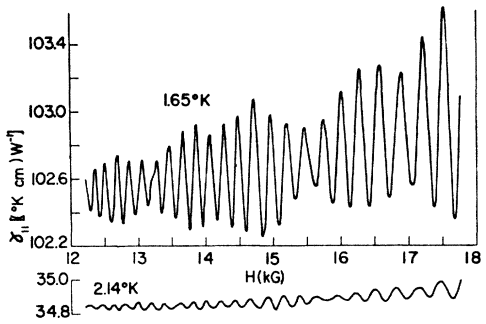

FIG. 12. The high-field thermomagnetoresistivity γ_{11} is seen to saturate at a constant value characteristic of heat conduction by the lattice except for a superimposed oscillatory component. The oscillations can be understood in terms of an electron-phonon scattering where the number of scattering electrons is affected by the Landau quantization.

10^{-7}W/cm °K was found at 1.6°K as compared with a measured $|\tilde{\lambda}_{11}''|\sim 10^{-4}$W/cm °K. Wiedemann-Franz-law oscillations could also be ruled out from phase considerations, as $\tilde{\gamma}_{11}$ and $\tilde{\sigma}_{11}$ should be π out of phase for the Weidemann-Franz law.

The possibility that the oscillations in γ_{11} might be a thermoelectric effect was also eliminated. The kinetic $\hat{\lambda}''$ and the experimental $\hat{\gamma}$ are related by $\hat{\lambda}''=\hat{\gamma}^{-1}(1+\hat{\epsilon}'^2\hat{\rho}^{-1}\hat{\gamma}^{-1}T)$. Thus a case could conceivably arise where an oscillation of γ_{11} would originate in the term $(\hat{\epsilon}'^2\hat{\rho}^{-1}\hat{\gamma}^{-1})_{11}$. In the present case, this is approximately $\epsilon_{21}'^2\sigma_{11}/\gamma_{11}$ and at 1.6°K, when the largest oscillations occur, represents a correction of 2.5% to the expression $\lambda_{11}''\approx(\hat{\gamma}^{-1})_{11}$. Oscillations in ϵ_{21}' and σ_{11} were no more than 2 and 1% of their respective gross effects. The oscillation in $\epsilon_{21}'^2\sigma_{11}/\gamma_{11}$ could thus be 0.125% of γ_{11} at most. As the measured effect is as high as 0.6% of γ_{11} at 1.6°K, this source of the effect is eliminated from further consideration.

A third and more likely source of the oscillations would be the occurrence of a magnetocaloric effect in the sweeping field. Such an effect, which would be an "isothermal" form of the magnetothermal oscillations reported by Kunzler *et al.*,[57] could possibly be found in bismuth, if not in antimony, and would, most significantly, be a direct measure of the grand canonical potential Ω.[58] There exists a clear experimental distinction between lattice conductivity and magnetocaloric oscillations. Since magnetocaloric effects appear only in changing fields, static-field measurements showing the field oscillatory behavior of Fig. 12 proved the effect definitely not of the magnetocaloric type.

Steele and Babiskin[59] observed oscillations of a similar nature in bismuth which they interpreted as being oscillations in the lattice conductivity. Unfortunately, no quantitative analysis of their data could then or can now be made, as their field was directed perpendicular to, rather than parallel to the trigonal axis; nor is it clear whether or not a point-by-point measurement was made.

Although an exact theory of oscillations in the lattice conductivity would be quite involved, it was found that a good (for oscillatory transport effects) quantitative description of our data could be obtained from simple considerations along the lines suggested by Steele and Babiskin.

If the usual two-band model is assumed, and the carriers of each band scatter the phonons independently of the other band, then $\gamma_g=\gamma_g{}^T+\gamma_g{}^W$. Equation (5) then implies a relation $\gamma_g=An_T{}^2+Bn_W{}^2$ at a given temperature. Thus, if the oscillations are due to fluctuations Δn_T of the Shoenberg ellipsoids, and the constraints $\Delta n_T=\Delta n_W$ and $n_T=n_W$ of two compensated bands are imposed, the relation $\Delta\gamma_g/\gamma_g=2\Delta n_T/n_T$ results. The effect was thus analyzed in terms of an expression of the form

$$|\tilde{\gamma}_g|/\gamma_g=\beta(|\tilde{n}|/n), \tag{22}$$

which relates the relative amplitudes of the thermal resistivity oscillations to the relative amplitudes of the number of carrier oscillations as defined by Eq. (17).

The value of β may depend on many factors. The simplest estimate begins from the condition $\Delta n_T=\Delta n_W$ and the fact $Z_T\neq Z_W$ from which it follows that $|\tilde{n}|/n\neq 2\Delta n_T/n_T$. Instead, the effective variation in the number of carriers for a two-band model is $\Delta n_T=\Delta n_W=[Z_T/(Z_T+Z_W)]\tilde{n}_W+[Z_W/(Z_T+Z_W)]\tilde{n}_T$ and since the detected oscillations $\tilde{n}$ are from the tilted ellipsoids only, one has $\Delta n_T=[\zeta_T/(\zeta_T+\zeta_W)]\tilde{n}$. Thus, from only these few considerations a value $\beta=1.2$ is to be expected. Values of $|\tilde{\gamma}_{11}|/\gamma_{11}$, $|\tilde{n}|/n$ and β are given in Table V. They fall in the range $0.5<\beta<2.1$, a rather remarkable proximity to the predicted value, in view of the oversimplifications made in obtaining that value.

A more exact theory of this effect may need to consider such details as the relative scattering efficiencies of electrons and holes on transverse and longitudinal phonons, and perhaps some aspect of phonon drag. Some of those features may be the explanation of the large temperature dependence ($|\tilde{\gamma}_{11}|$ increases tenfold between 2.1 and 1.6°K), but it should also be pointed

TABLE V. Measured relative amplitudes $|\tilde{\gamma}_{11}|/\gamma_{11}\times 100\%$ of oscillations in the lattice thermal resistivity γ_{11g} compared to relative amplitudes at the same two fields and temperatures of the fluctuation $\tilde{n}$ in the number of carriers of the tilted ellipsoids. Good agreement is found in the parameter β computed from the relation $|\tilde{\gamma}_g|/\gamma_g=\beta|\tilde{n}/n|$ and theoretically of order unity. The values of $|\tilde{n}/n|$ were computed from Eq. (17).

T(°K)	$\lvert\tilde{\gamma}_{11}\rvert/\gamma_{11}$ ×100%	$\lvert\tilde{n}\rvert/n$ ×100%	β	H(kG)
1.65	0.20	0.15	1.3	13.0
	0.61	0.29	2.1	17.6
2.14	0.06	0.11	0.54	13.0
	0.15	0.24	0.62	17.6

[57] J. E. Kunzler, F. S. L. Hsu, and W. S. Boyle, Phys. Rev. **128**, 1084 (1962).

[58] M. Ya. Azbel, Zh. Eksperim. i Teor. Fiz. **39**, 878 (1960) [English transl.: Soviet Phys.—JETP **12**, 608 (1961)].

[59] M. C. Steele and J. Babiskin, Phys. Rev. **98**, 359 (1955).

out that the n^2 proportionality of γ in Eq. (5) is already derived from a partial dependence of the scattering on the density of states Z, which in turn depends on n. With $|\tilde{Z}|/Z \gg |\tilde{n}|/n$ and different temperature contributions for those terms, it appears possible that the large temperature dependence would be just the expected behavior of the simple electron-phonon N scattering.

V. CONCLUSIONS

This study has brought out some special features of antimony for the observation of a nearly pure electron-phonon normal-process scattering and its effects on the different transport coefficients. This conclusion was first confirmed by a T^7 dependence of the ratio of the lattice thermal and ideal electrical conductivities. The apparent disagreement between the individual conductivities leading to the ideal T^7 law and the standard electron-phonon N-scattering theory could also be explained plausibly through an extension of the Grüneisen theory of metals to the case of semimetals.

In the low-field study of the galvanomagnetic coefficients, the relaxation-time concept was found to have wider applicability than generally supposed. All of the kinetic coefficients were described quite well by the standard two-band Sondheimer-Wilson theory based on the existence of a time of relaxation, with two exceptions: (1) Low-field data for σ_{11} and σ_{12} were individually very well described by the theory, but a consistent set of parameters could not be assigned to both conductivities. This was one of several features of the transport data thought to be an indication of the presence of a third band. (2) The field dependence of ϵ_{11}'' was anomalous. Phonon drag may have been responsible for the anomaly.

The existence of the nearly pure electron-phonon N scattering in both electrical and thermal processes resulted in an analysis of the large and temperature-dependent Nernst-Ettinghausen density of states in terms of a very simple phonon-drag theory. A successful explanation of the data in this way proved the existence of a large phonon-drag effect in a range of temperatures where it is generally expected to be negligible, and may have implications toward the large density-of-states values reported for semimetals in general.

The amplitudes and phases of the oscillatory electrical and thermoelectric coefficients did not fit any of the available theories particularly well, but the failure was unusual in that several of the theoretical amplitude predictions were greater than the measured effect. The supposition that large predicted amplitudes could be decreased to the measured values by the inclusion of a collision broadening term could not be justified with a reasonable value of the cutoff time.

Oscillations in the nearly constant thermal resistivity at high field were concluded to be a consequence of oscillations in the lattice conductivity. Comparison of measured amplitudes of the oscillations in the thermal resistivity with the theoretical relative amplitudes of the carrier density oscillation led to the conclusion that oscillations in the lattice conductivity were due to scattering of the lattice wave by Landau-quantized electrons with the generally accepted n^2 proportionality, characteristic of the electron-phonon N scattering.

ACKNOWLEDGMENT

We are indebted to Dr. G. N. Rao and Dr. N. H. Zebouni for their assistance in the different phases of this work, to Dr. G. Hussey for reading the manuscript, and also to the members of the Low Temperature group, most particularly to our late friend A. Venkataram, for the generous help given us in the experimental part of this work.